Synthesis and photophysical properties of a highly fluorescent azo derivative

Li-Hong Liu, Keitaro Nakatani and Eléna Ishow*

Received (in Montpellier, France) 30th January 2009, Accepted 27th March 2009
First published as an Advance Article on the web 16th April 2009
DOI: 10.1039/b902018g

A highly fluorescent and photochromic azo derivative has been obtained by linking in a covalent manner a red-emitting squaraine unit to an azo dye. The bifunctional molecule exhibits uncoupled chromophores in the ground state allowing for the specific addressing of the azo photoisomerization and squaraine emission. Photosensitization of the squaraine unit by exciting the azo moiety in its UV absorption band has been obtained. Such an unusual energy transfer has been modulated by changing the solvent from chloroform to toluene. This led to a dramatic enhancement of the emission quantum yield Φ_f (from 0.35 up to 0.71) without affecting the photoisomerization process. Strong competitive π-stacking interactions between toluene and squaraine have been put forward to interpret the emission changes.

Introduction

The concomitant association of photochromic and fluorescent entities has been boosted in the very recent years by the promising development of high density optical memories,[1] photoswitchable light emitting organic diodes,[2] and probe photoactivation for live-cell imaging.[3] The working principle of these photonic devices relies on the modulation of the fluorophore emission intensity by the photochromic reaction which advantageously occurs in a reversible and contact-free manner in less than a few picoseconds.[4] In his pioneering work, Irie *et al.* devised a bifunctional system made of a diarylethene unit linked through an alkyl spacer to a fluorescent moiety.[5] This latter was carefully chosen so that its radiative excited state could deactivate the closed form following a Förster energy transfer mechanism the efficiency of which was governed by the spectral overlap between the fluorophore emission band and the absorption band of the closed photoisomer. Since then, numerous studies have been performed on diarylethene,[6] spirooxazine[7] and spiropyrane[8] derivatives aiming at improving the quenching mechanism efficiency and reducing the risks of retrocyclization upon light reabsorption by the closed forms. Curiously little attention has been paid to the combination of fluorophores with azo derivatives. These latter photochromes actually exhibit fascinating properties as potential photoactivable nanomotors due to their photoorientation and photomigration abilities when subjected to polarized light.[9] Attaching a fluorescent tail to an azo unit would open new horizons on the reversible nanostructuration of fluorescent patterns and optical manipulation of fluorescent biolabels at the molecular level.

Such an association is however facing a picosecond photoisomerization process of the azo unit which mostly leads to the very efficient emission quenching of neighboring fluorophores.[10] Biologists have benefited from this effect to follow the dynamics of molecular beacons or the pairing of two DNA complementary strands containing an azo and emissive units by monitoring the emission changes as a function of the azo–fluorophore distance.[11] Recently several groups reported the formation of fluorescent azo derivatives in solution[12] or in the solid state upon aggregation.[13] Nevertheless fluorescence appeared at the expense of the photoisomerization process which was totally suppressed.

To circumvent the antinomic properties of fluorescence and photoisomerization in an azo-containing molecule, we have earlier proposed an approach involving the introduction of a fluorophore emitting at low energy, far from the azo absorption band.[14] We came up with a squaraine unit known for its remarkable emission properties characterized by a high emission quantum yield ($\Phi_f > 0.7$), a sharp and narrow emission spectrum peaking in the red region ($\lambda_{em} > 640$ nm) and a large photostability, hence its multifold use for applications spanning from photonic materials to ion detection.[15] Its attachment to the Disperse-Red 1, a push–pull azo compound, was accomplished by using an aminoethyl linker whose saturated character ensured partial electronic disconnection between the two functional entities. A short spacer was preferred over longer alkyl chains to restrain deleterious folding which is likely to lead to intramolecular π–π stacking of the azo and squaraine backbones and form a radiationless species.[16] The bifunctional compounds we synthesized following these guidelines did fluoresce and photoisomerize. They suffer however from an undesirable photoinduced electron transfer (PET) in the excited state from the nitrogen atom of DR1, hence the incorporated squaraine unit underwent a large decrease in Φ_f down to 0.1.

We want to show herein that replacing the nitrogen atom with oxygen allowed us to notably improve the emission properties of the bifunctional molecule while the azo unit keeps photoisomerizing in solution. The incorporation of the less electron-donating oxygen atom led not only to a decrease

PPSM-UMR CNRS 8531, ENS Cachan, PRES-UniverSud Paris, 61 Avenue du Président Wilson, Cachan Cedex, 94 325, France. E-mail: elena.ishow@ens-cachan.fr; Fax: 33-1-4740-2454; Tel: 33-1-1-4740-7660

in the PET phenomenon but also to the blue shift of the azo absorption maximum, which limits the risks of energy transfer from the squaraine to the azo unit. Influence of the solvent onto the emission properties has been evidenced, leading to a considerable fluorescence enhancement through competitive π–π interactions with the squaraine unit without affecting the azo photoisomerization process.

Experimental

Materials and synthesis

^{1}H and ^{13}C NMR spectra were recorded on a Bruker 300 MHz spectrometer, and chemical shifts δ were reported in ppm relative to TMS and referenced to the residual solvent. Mass spectra were obtained with a MALDI-TOF Perseptive Biosystems instrument. Bis[4-(dibutylamino)phenyl]squaraine **bsq**,[17] 4-hydroxy-4′-nitroazobenzene **1**[18] and 1-(*p*-dibutylaminophenyl)-2-hydroxycyclobuten-3,4-dione **4**[19] were synthesized according to literature procedures.

N-(2-Tosyloxyethyl)-*N*-ethylaniline 2

A mixture of *N*-ethyl-*N*-hydroxyethylaniline (0.83 g, 5 mmol) and freshly distilled triethylamine (1.0 mL, 7.5 mmol) dissolved in anhydrous dichloromethane (50 mL) was cooled to 0–5 °C under argon. Tosylate chloride (1.40 g, 7.5 mmol) was added portionwise over 30 min. The mixture was kept stirring under argon at 0–5 °C for 6 h and poured into an ice–water mixture (50 mL). The crude product was extracted with dichloromethane. The combined organic layers were washed with brine and dried over anhydrous magnesium sulfate. Removal of the solvent under vacuum and purification by silica gel column chromatography using a 2 : 1 mixture of petroleum ether–ethyl acetate as the eluent gave **2** as a colorless oil (0.71 g, yield 44%). ^{1}H NMR (300 MHz, $CDCl_3$): δ 7.76 (d, J = 8.3 Hz, 2 H), 7.29 (d, J = 8.7 Hz, 2 H), 7.18 (dd, J = 7.3 Hz, 7.8 Hz, 2 H), 6.68 (dd, J = 6.9 Hz, 7.3 Hz, 1 H), 6.56 (d, J = 8.0 Hz, 2 H), 4.15 (t, J = 6.5 Hz, 2 H), 3.58 (t, J = 6.5 Hz, 2 H), 3.32 (q, J = 7.0 Hz, 2 H), 2.43 (s, 3 H), 1.11 (t, J = 6.9 Hz, 3 H) ppm; ^{13}C NMR (75 MHz, $CDCl_3$): δ 146.9, 145.0, 132.7, 129.9, 129.4, 127.9, 116.5, 111.8, 67.0, 48.9, 45.5, 21.7, 12.2 ppm; HRMS (MALDI-TOF): m/z (%) [M + H$^+$] calc. for $C_{17}H_{22}NO_3S$ 320.1320, found 320.1309 (100); Elemental analysis, Found: C, 63.91; H, 6.89; N, 4.42. Calc. for $C_{17}H_{22}NO_3S$: C, 63.92; H, 6.63; N, 4.39%.

4-[2-(*N*-Ethyl-*N*-phenylamino)ethyloxy]-4′-nitroazobenzene 3

A mixture of compound **2** (0.7 g, 2.2. mmol), 4-hydroxy-4′-nitroazobenzene **1** (0.49 g, 2 mmol) and potassium carbonate (0.42 g, 3 mmol) in anhydrous dimethylformamide (4 mL) was stirred under argon at 100 °C for 24 h. After cooling to room temperature, the reaction mixture was poured under stirring into a 1 mol L^{-1} hydrochloric acid solution (20 mL) and the solid was filtered off. The residue was washed with water to neutrality, and recrystallized from ethyl acetate–acetonitrile to give compound **3** as shiny orange–red flakes (0.66 g, 77%); mp 113 °C; ^{1}H NMR (300 MHz, $CDCl_3$): δ 8.36 (d, J = 8.8 Hz, 2 H), 7.98 (d, J = 9.2 Hz, 2 H), 7.95 (d, J = 9.2 Hz, 2 H), 7.25 (dd, J = 7.3, 8.8 Hz, 2 H), 7.02 (d, J = 9 Hz, 2 H), 6.75 (d, J = 8.8 Hz, 2 H), 6.71 (t, J = 7.3 Hz, 1 H), 4.23 (t, J = 6.2 Hz, 2 H), 3.78 (t, J = 6.2 Hz, 2 H), 3.50 (q, J = 7.0 Hz 2 H), 1.22 (t, J = 7.0 Hz, 3 H) ppm; ^{13}C NMR (75 MHz, $CDCl_3$): δ 162.3, 155.9, 148.2, 147.4, 146.9, 129.4, 125.5, 124.6, 123.0, 116.2, 114.8, 111.8, 65.9, 49.5, 45.7, 12.2 ppm; HRMS (MALDI-TOF): m/z (%) [M + H]$^+$ calc. for $C_{22}H_{23}N_4O_3$: 391.1772, found: 391.1770 (100); λ_{max}(chloroform, *E*-isomer)/nm 375 (log ε 4.45).

4-[2-(*N*′-{4′-[4-(Dibutylaminophenyl)squaraine]phenyl}-*N*′-ethylamino)ethyloxy]-4′-nitroazobenzene 5 (AzoO-bsq)

Compound **3** (0.19 g, 0.5 mmol) was stirred overnight with 1-(*p*-dibutylaminophenyl)-2-hydroxycyclobuten-3,4-dione **4** (0.18 g, 0.6 mmol) in the presence of tributylorthoformate (2 mL) in refluxing propan-2-ol (10 mL) under argon. After cooling down and storage at 0 °C for 12 h, the precipitate was filtered off and washed with methanol to yield a dark blue solid. Purification on column chromatography (silica gel, toluene–ethyl acetate 2 : 8) provided compound **5** as a fine dark blue powder (98 mg, 29%); mp 184.5 °C; ^{1}H NMR (300 MHz, $CDCl_3$): δ 8.39 (d, J = 8.8 Hz, 2 H), 8.38 (d, J = 9.2 Hz, 2 H), 8.36 (d, J = 9.2 Hz, 2 H), 7.98 (d, J = 8.8 Hz, 2 H), 7.96 (d, J = 9.2 Hz, 2 H), 7.02 (d, J = 9.2 Hz, 2 H), 6.84 (d, J = 9.2 Hz, 2 H), 6.73 (d, J = 9.5 Hz, 2 H), 4.31 (t, J = 5.3 Hz, 2 H), 3.94 (t, J = 5.2 Hz, 2 H), 3.67 (q, J = 7.0 Hz, 2 H), 3.44 (t, J = 7.7 Hz, 4 H), 1.65–1.60 (m, 4 H), 1.44–1.01 (m, 4H), 1.32 (t, J = 7.0 Hz, 3 H), 0.99 (d, J = 7.4 Hz, 6 H) ppm; ^{13}C NMR (75 MHz, $CDCl_3$): δ 187.3, 183.2, 161.7, 155.9, 154.0, 152.6, 148.3, 147.2, 133.7, 132.8, 125.6, 124.6, 123.1, 120.3, 119.5, 114.8, 112.4, 112.2, 65.7, 51.2, 49.6, 46.4, 29.5, 20.1, 13.7, 12.3 ppm; HRMS (MALDI-TOF): m/z (%) [M + H]$^+$ calc for $C_{40}H_{44}N_5O_5$: 674.3342, found: 674.3322 (100); λ_{max}(chloroform, *E*-isomer)/nm 375 (log ε 4.47), 636 (5.49).

Measurements

UV-Vis spectra were recorded on a Varian Model Cary 5 E spectrophotometer. Melting points were measured by using a Perkin Elmer Pyris Diamond Differential Scanning Calorimeter. Corrected emission spectra were obtained using a Spex Fluorolog 1681 spectrofluorometer. Fluorescence quantum yields were determined from solution of bis[4-(dibutylamino)-phenyl]squaraine absorbing equally at the excitation wavelength. Fluorescence intensity decays were measured by the time-correlated single-photon counting method with a picosecond laser excitation at 495 nm provided by a Spectra-Physics setup composed of a titanium-sapphire Tsunami Laser pumped by an argon ion laser, and doubling LBO crystals. Light pulses were selected by an optoacoustic crystal at a repetition rate of 4 MHz. Fluorescence photons were detected at 630 nm through a monochromator by a Hamamatsu MCP photomultiplier R3809U connected to a constant-fraction discriminator. Pulse deconvolution was performed from the time profile of the exciting pulse recorded under the same conditions by using a Ludox solution. Photoisomerization kinetics was recorded on magnetically stirred solutions using a continuous Hg–Xe lamp (Hamamatsu, LC8-06) equipped with an optical fiber and a 366 nm interferential filter (5.9 mW cm^{-2}) as a pump source while simultaneous probing

was performed with a continuous Xe lamp (450 W) and a CCD camera coupled with a spectrometer (Princeton Instruments).

Computations

TD-DFT calculations were conducted using the Becke's three-parameter hybrid functional and the correlation functional of Lee, Yang and Parr (B3LYP)[20] with a 6-31G(d) basis set[21] as implemented in the GAUSSIAN 03 package.[22] Illustrations were obtained with GaussView 3.0.

Results and discussion

Synthetic strategy and absorption properties

The synthesis of the bifunctional compound **5** (**azoO-bsq**) proceeded after a three-step sequence allowing us to also generate the fluorescent **bsq** and photochromic **azoO** model compounds (Scheme 1).

Model compounds are mandatory to value the spectroscopic properties of the photoactive units once they are covalently connected in **azoO-bsq**. 4-Hydroxy-4′-nitroazobenzene **1** was first synthesized through the azo coupling reaction between phenol and 4-nitroaniline in hydrochloric acid solution. The azo compound **1** was reacted further with the previously tosylated *N*-ethyl-*N*-(2-hydroxyethyl)phenylamine **2** following a nucleophilic substitution in anhydrous dimethylformamide in the presence of potassium carbonate to give a red compound **3** in 77% yield. Finally, the azo compound **3**, serving also as the model photochrome **azoO**, was coupled to the dibutylsquarate **4**, prepared after a three-step procedure, in refluxing propan-2-ol with tributylorthoformate. The bifunctional **azoO-bsq** was obtained as a dark blue powder in 29% yield. Following the same reaction conditions, the fluorescent model compound bis[4-(dibutylamino)phenyl]squaraine **bsq** was generated from dibutylsquarate and *N*,*N*-dibutylphenylamine and obtained as a shiny gold–green powder.

UV-vis absorption and emission properties

The UV-vis absorption spectrum of **azoO-bsq** in chloroform exhibits two bands peaking in the UV at 373 nm and in the visible at 633 nm. These bands have been ascribed to transitions located on the azo and the squaraine units respectively from comparison with the absorption spectra of the model compounds (Fig. 1).

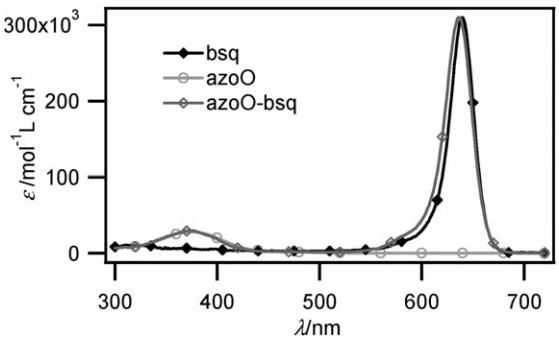

Fig. 1 UV-vis absorption spectra of the bifunctional compound **azoO-bsq** and model compounds **bsq** and **azoO** in chloroform solution.

Since the squaraine band is *ca.* ten times as high as the azo one absorbing in the UV, the solution appears bright blue (Fig. 2).

These maxima correspond almost exactly in energy to those of the separate photochrome **azoO** and fluorophore **bsq** models absorbing at 373 and 640 nm, respectively. Moreover the sum in a ratio 1 : 1 of the molar absorption coefficients of the model compounds nearly corresponds to the values established for **azoO-bsq**. We can thus conclude that the azo and squaraine units do not significantly interact in the ground state. Replacing a dialkylamino moiety with an alkoxy one has led to a 100 nm hypsochromic shift of the azo band due to a strong decrease in the push–pull strength. This allowed us to photoaddress each unit independently and investigate the emission and photochromic properties of the whole.

The emission properties were first investigated in dilute chloroform solution such that the absorbance of the squaraine unit was always kept lower than 0.1 to minimize the risks of emission reabsorption and intermolecular aggregation. Excitation of **azoO-bsq** in the squaraine-located band at 590 nm led to a strong and narrow red emission centered at 648 nm (Fig. 3). This fluorescence was found to be slightly blue-shifted with regard to **bsq** emitting at 653 nm.

When the excitation was performed in the azo UV band of **azoO-bsq** around 375 nm, the same red emission was observed. Its magnitude was twice as large as that obtained for a solution of **bsq** of equal concentration, and excited at the same wavelength. Two isoabsorbing wavelengths in the azo and squaraine bands, namely at 377 and 590 nm were considered.

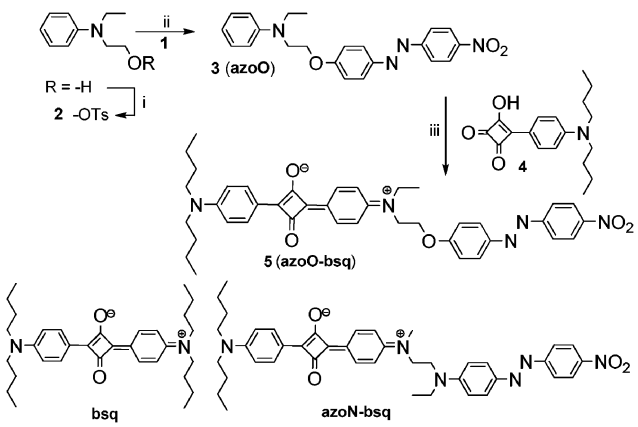

Scheme 1 Synthetic pathway to **azoO-bsq**. *Reagents and conditions*: (i) tosylate chloride, triethylamine, CH_2Cl_2, 0 °C, 6 h; (ii) 4-hydroxy-4′-nitroazobenzene **1**, dimethylformamide, K_2CO_3, 100 °C, 24 h; (iii) tributylorthoformate, dibutylsquarate **4**, propan-2-ol, 83 °C, 12 h.

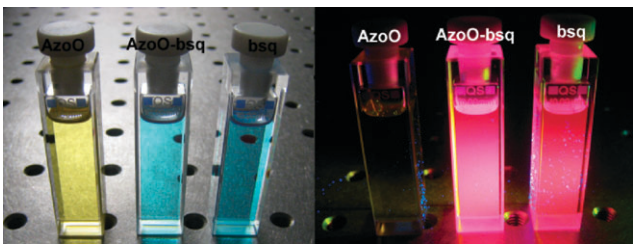

Fig. 2 **AzoO**, **azoO-bsq** and **bsq** in chloroform solution: left: absorption, right: emission; λ_{exc} = 547 nm (Hg–Xe lamp).

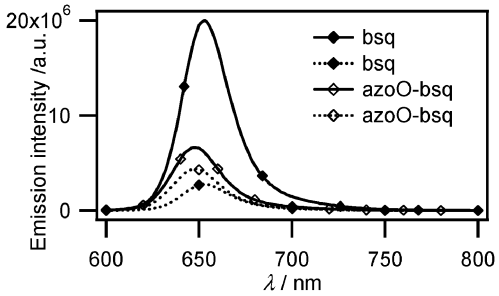

Fig. 3 Emission spectra of **bsq** and **azoO-bsq** in chloroform solution. Excitation was performed at 590 nm (bold line) and 377 nm (dashed line).

After subtracting the UV-excited squaraine contribution, the squaraine photosensitization by the azo moiety was assessed to represent 25% of the intensity obtained upon excitation at 590 nm. The azo participation in the emission process was confirmed by recording an excitation spectrum at 660 nm. Two bands, characteristic of the azo and squaraine absorption ranges, were obtained. The intensity of the azo band was significantly reduced to 60% of the azo absorption band in accord with the partial photosensitization effect reported above (Fig. 4).

The fluorescence quantum yield ϕ_f was valued to 0.35 after excitation at 590 nm, which is significantly larger than that of the amino analogue **azoN-bsq** (ϕ_f = 0.1). The emission enhancement in **azoO-bsq** was reasonably attributed to the reduced electron-donating character of the ethoxy group, which is less prone to photoinduced electron transfer than the amino moiety in **azoN-bsq**.

When chloroform was replaced with toluene, a dramatic enhancement of ϕ_f up to 0.71 was observed for **azoO-bsq** (up to 0.29 for **azoN-bsq**). In contrast, the emission quantum yield of **bsq** only increased from 0.92 to 1.00. This enhancement was accompanied by a notable decrease of the squaraine's photosensitization effect by exciting the azo unit, down to 16% of the signal obtained after direct excitation in the squaraine-based transition. At this step, both a Dexter and/or Förster energy transfer processes could be envisaged to explain the observed photosensitization effect. This latter is all the more surprising since the azo photoisomerization reaction occurs in the picosecond time range and can efficiently deactivate close emitters.

Therefore we conducted TD-DFT calculations on **azoO-bsq** in the gas phase (B3LYP/6-31G(d)) to gain a qualitative

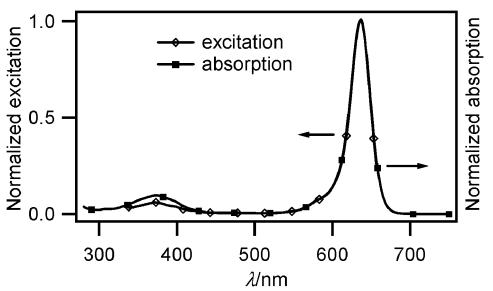

Fig. 4 Normalized excitation (λ_{em} = 660 nm) and absorption spectra of **azoO-bsq** in chloroform solution.

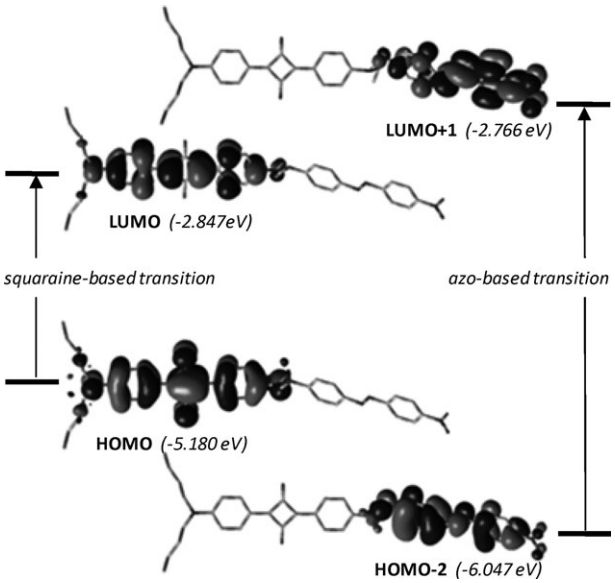

Fig. 5 DFT-computed molecular orbitals of **azoO-bsq** in the gas phase with the correlation functional B3LYP and a 6-31G(d) basis set.

insight into the two energy transfer mechanisms which respectively depend on the molecular orbital overlap (Dexter) and the transition dipole moments (Förster) attached to the azo and squaraine units. The computations provided two distinct π–π* transitions specifically located on the azo (HOMO−2 → LUMO + 1) and squaraine parts (HOMO → LUMO) (Fig. 5).

These transitions matched fairly well both the azo- and squaraine-centered bands of the experimental absorption spectrum. The involved frontier MOs present a lateral π-overlap, which is a pre-requisite for a Dexter energy transfer to occur between the azo and squaraine units. As for the Förster energy transfer, the orientation of the transition dipole moments related to the azo and squaraine moieties appears to be quite favorable. The calculations showed that their vectors point along the main axis of the corresponding chromophore, and form a 16° angle in the minimized elongated geometry. However, the donor emission and acceptor absorption spectra should display substantial spectral overlap, not found in our systems. By comparison with **bsq**, the squaraine absorption in **azoO-bsq** at 375 nm has been inferred to be six times as low as the azo one. If a Förster energy transfer operates, the oscillator strength of the squaraine acceptor should be large enough to compensate the weak spectral overlap between the donor (azo) and the acceptor (squaraine) moieties as well as the subpicosecond radiative decay of the azo S_2 and S_1 excited states.[23] We indeed found by computations an oscillator strength f of about 1.47 for the squaraine-based HOMO → LUMO transition in agreement with the values reported in literature. Finally, the considerable changes caused by toluene onto the emission properties of **azoO-bsq** could be interpreted as a strong solvation effect of the π-conjugated backbone, producing remote units and "*electronic insulation*" of the squaraine. Consequently, the emission of the squaraine increases while its photosensitization by exciting the azo unit diminishes. These observations allow us to suggest that the energy transfer from the azo to the squaraine units may rather

Table 1 UV-vis spectroscopic data (absorption, emission) of compounds **azoO**, **azoO-bsq**, **azoN-bsq** and **bsq**, rate constants of the back thermal reaction *Z*–*E* and minimum conversion yields for the photochromic azo compounds in toluene solution

	λ_{max}^{abs}/nm	λ_{max}^{em}/nm	ϕ_f[a]	τ_f[b]/ns	$10^{-4}k/s^{-1}$	η^f (%)
azoO	375	—	—	—	3.2[d]	67
azoO-bsq	375	644	0.71	0.26[c]	4.1[d]	14
	632			1.96	—	—
azoN-bsq	463	649	0.29	0.70[c]	115[e]	29
	635			1.24	—	—
bsq	636	647	1.00	2.31	—	—

[a] λ_{exc} = 590 nm with **bsq** as a standard. [b] λ_{exc} = 495 nm, λ_{em} = 630 nm. [c] Major component of the biexponential lifetime decay: 99.5% (**azoO-bsq**), 89% (**azoN-bsq**). [d] Measured in isoabsorbing toluene solutions at 366 nm and kinetics recorded at 375 nm. [e] Kinetics recorded at 460 nm after excitation at 488 nm. [f] Assuming no absorption from the *Z* photoisomers.

follow a dipole–dipole coupling mechanism. However, the flexibility of the ethyl linker allows both units to freely rotate in solution, leading to a decrease in the dipole–dipole coupling. In the same way, the spatial overlap can severely drop and so reduce the efficiency of the through-bond electron-exchange mechanism. Therefore both the Dexter and the Förster mechanisms may operate, each depending on the experimental conditions involved.[24]

Finally, measurements of the lifetime were conducted at λ_{exc} = 495 nm to avoid excitation in the azo band and risks of photoisomerization. Emission was recorded at λ_{exc} = 630 nm by using a monochromator to avoid detection of solvent-squaraine excited states emitting beyond 660 nm.[25] In chloroform and toluene solutions, the fluorescence decay could be modeled by a biexponential lifetime. The major component was found at τ_1 = 0.68 ns (93%) in chloroform, and evolved to τ_1 = 1.96 ns (99.5%) in toluene solution, close to the 2.31 ns monoexponential lifetime measured for **bsq** (Table 1). The absence of fluorescent impurities was carefully checked at this stage. Furthermore, the synthetic pathway adopted to generate the asymmetric squaraine rules out the accumulation of other squaraine byproducts. The longer decay observed in toluene agrees with the enhanced emission quantum yield reported above. A reasonable explanation for the presence of two lifetimes for **azoO-bsq** and their solvent-dependency may rely on the flexible ethyl spacer. The molecule can adopt a variety of conformations in solution enabling remote positions of the squaraine unit from the azo one (hence the long lifetime especially in toluene) as well as close vicinity of the azo and squaraine units to form a short-lived excited π–π adduct.

Photochromic properties

Measurements of the azo photochromic behavior require solutions of concentration above 1×10^{-5} mol L^{-1} to ensure adequate detection sensitivity. This concentration range is likely to give rise to squaraine dimerization characterized by strong association constants around 10^5 mol^{-1} L.[26] Choice of the solvent was therefore crucial to provide an accurate picture of the photochromic properties of the "isolated" molecule. Whereas toluene and chloroform solutions gave the same absorption ratio of 10 between the maxima of the squaraine and azo units, this ratio fell to 2.5 in acetonitrile. Simultaneously the half-bandwidth of the squaraine-located transition broadened from 27 nm (30 nm) to 34 nm when going from toluene (chloroform) to acetonitrile. These spectral observations evidence the fact that toluene and chloroform limit the risks of squaraine aggregation at high concentration by exerting disruptive π–π interactions. Moreover, toluene displays moderate polarity, known to considerably influence the back thermal reaction of the photogenerated *Z*-isomers, and has largely been used for other azo derivatives, which facilitates kinetics comparisons.

Photoisomerization was carried out with a continuous Hg–Xe lamp source equipped with a 366 nm bandpass filter. Absorption changes were probed *in situ* by using a low-power white-light source. Solutions of **azoO-bsq** and **azoO** with identical absorbance at the azo-centered band maximum were prepared to permit straightforward comparison between both compounds and discard artifacts due to distinct light absorption or concentration effects. The depletion of the *E*-isomer absorption band was neatly observed at 375 nm while a new weak band, characterizing the formation of the *Z*-isomer, appeared at 482 and 463 nm for **azoO-bsq** and **azoO**, respectively (Fig. 6). Two isosbestic points were observed, the first one being formed around 330 nm (327 and 331 nm for **azoO-bsq** and **azoO**, respectively) and the second one in the visible at 425 nm for **azoO-bsq** and 444 nm for **azoO**. This indicates that the azo units in the *E*- and *Z*-isomers behave in a similar way for both the bifunctional and the azo compounds, hence the **azoO-bsq** species exists in a more probable monomeric form.

The back-thermal relaxation kinetics for both compounds was determined at the depletion minimum at 375 nm once the photostationary state was reached. The differential absorbance time-evolution could be modeled by a monoexponential law in accord with the first-order $Z \rightarrow E$ thermal reaction in a fluid and isotropic medium, $[E] = [E]_0 + \{[E]_P - [E]_0\}\exp(-kt)$ where k designates the reaction rate constant and $[E]_0$ and $[E]_P$ the concentrations of the *E*-isomer before irradiation and at the photostationary state, respectively (Fig. 7). **AzoO-bsq** was found to relax slightly faster than **azoO** with k around 4.1×10^{-4} against 3.2×10^{-4} s^{-1} respectively. This process is almost two orders of magnitude slower than that for **azoN-bsq** as expected from the less polar character of the N=N bond in **azoO-bsq**.[27] The similarity between the rate constants proves

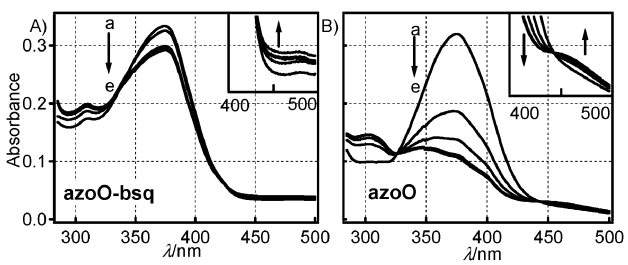

Fig. 6 Absorption changes of 1×10^{-5} mol L^{-1} solutions of **azoO-bsq** and **azoO** in toluene after irradiation at 366 nm (5.9 mW cm^{-2}). Recorded at time for A: **azoO-bsq**: (a) 0 s, (b) 5 s, (c) 30 s, (d) 60 s, (e) 120 s, and for B: **azoO**: (a) 0 s, (b) 5 s, (c) 20 s, (d) 40 s, (e) 60 s.

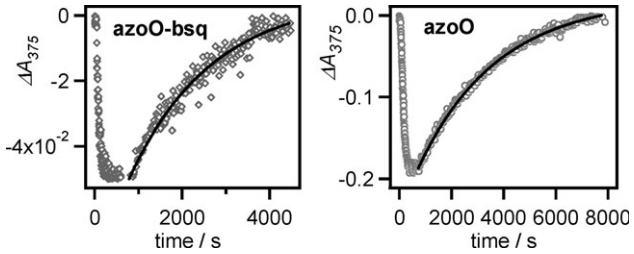

Fig. 7 Kinetics of the back thermal relaxation of 1×10^{-5} mol L^{-1} solutions of **azoO-bsq** and **azoO** in toluene after irradiation at 366 nm (5.9 mW cm^{-2}). Absorption changes followed at 373 nm.

that the photoisomerization reaction is not fundamentally impaired by the presence of the squaraine unit.

The main difference stems from the minimum conversion yield η which has been estimated to be 14 and 67% for **azoO-bsq** and **azoO** from the absorbance depletion at 375 nm at the photostationary state. It is noteworthy that neither η nor the rate constants k significantly changed when the photoisomerization was conducted in chloroform (k was kept almost constant at 4.2×10^{-4} and 4.5×10^{-4} s^{-1} for **azoO-bsq** and **azoO**, respectively). The large discrepancy in η is to be connected to the photosensitization effects reported above. Indeed, it is reasonable to envisage that part of the energy absorbed by the azo unit is transferred to the squaraine unit at the expense of the photoisomerization process, hence a lower conversion yield. This prompted us to investigate the influence of photoisomerization onto the fluorescence spectra. It turns out that the emission maximum was almost unaffected with a 7% band decrease only while the squaraine absorption band maximum diminished by 1% at the photostationary state. This feature shows that the photoaccumulation of *Z*-isomers does not significantly influence the fluorescence signal of the squaraine emitter contrarily to azo-functionalized semiconductive polymers reported in the literature.[28]

Conclusions

We have described the synthesis and photophysical properties of a new bifunctional molecule combining the photochromic behavior of an azo derivative with the strong fluorescence of a squaraine unit. The introduction of a short and saturated spacer between the photochromic and fluorescent groups avoids significant folding in solution leading to deleterious intramolecular aggregation of the azo and squaraine π-conjugated backbones. Photoisomerization of the azo unit reversibly operates without affecting the fluorescence of the squaraine unit, which makes this system attractive for investigating the photoinduced motion of the azo unit at the single molecule level. The *E* to *Z* minimum conversion was found to be 20% of the azo model compound. The diminution in the photoisomerization efficiency has been assigned to an unusual energy transfer from the azo to the squaraine unit leading to a photosensitization of the latter. Such an energy transfer and the squaraine unit's emission appear to strongly depend on the solvent. The dramatic enhancement of the fluorescence quantum yield up to 0.71 in toluene has been interpreted in terms of competitive solvent π-stacking effects, which made the squaraine interact less with the vicinal azo π-backbone moiety and move away from it. Temperature-dependent experiments and transient absorption spectroscopy measurements to characterize the energy transfer dynamics are currently under study. They will be coupled with single molecule fluorescence investigations to track the azo unit's motion during the photoisomerization process.

References

1 (*a*) M. Irie, T. Fukaminato, T. Sasaki, N. Tamai and T. Kawai, *Nature*, 2002, **420**, 759; (*b*) M. Tomasulo, S. Giordani and F. M. Raymo, *Adv. Funct. Mater.*, 2005, **15**, 787–794.
2 (*a*) Z. Zhang, X. D. Liu, Z. Y. Li, Z. I. Chen, F. Q. Zhao, F. I. Zhang and C. H. Tung, *Adv. Funct. Mater.*, 2008, **18**, 302–307; (*b*) C. C. Corredor, Z.-H. Huang, K. D. Belfield, A. R. Morales and M. V. Bondar, *Chem. Mater.*, 2007, **19**, 5165–5173.
3 (*a*) L. Zhu, W. Wei, M.-Q. Zhu, J. J. Han, J. K. Hurst and A. D. Q. Li, *J. Am. Chem. Soc.*, 2007, **129**, 3524–3526; (*b*) M. Andresen, A. C. Stiel, S. Trowitzsch, G. Weber, C. Eggeling, M. C. Wahl, S. W. Hell and S. Jakobs, *Proc. Natl. Acad. Sci. U. S. A.*, 2007, **104**, 13005–13009; (*c*) S. Habuchi, R. Ando, P. Dedecker, W. Verheijen, H. Mizuno, A. Miyawaki and J. Hofkens, *Proc. Natl. Acad. Sci. U. S. A.*, 2005, **102**, 9511–9516.
4 F. Raymo and M. Tomasulo, *J. Phys. Chem. A*, 2005, **109**, 7343–7452.
5 T. Fukaminato, T. Sasaki, T. Kawai, N. Tamai and M. Irie, *J. Am. Chem. Soc.*, 2004, **126**, 14843–14849.
6 (*a*) T. Fukaminato, T. Umemoto, Y. Iwata, S. Yokojima, M. Yoneyama, S. Nakamura and M. Irie, *J. Am. Chem. Soc.*, 2007, **129**, 5932–5938; (*b*) G. Jiang, S. Wang, W. Yuan, L. Jang, Y. Song, H. Tian and D. Zhu, *Chem. Mater.*, 2006, **18**, 235–237.
7 X. H. Sheng, A. D. Peng, H. B. Fu, Y. Y. Liu, Y. S. Zhao, Y. Ma and J. N. Yao, *Nanotechnology*, 2007, **18**, 145707.
8 T. Tomasulo, E. Deniz, R. J. Alvarado and F. M. Raymo, *J. Phys. Chem. C*, 2008, **21**, 8038–8045.
9 (*a*) M. Yamada, M. Kondo, J. I. Mamiya, Y. Yu, M. Kinoshita, C. J. Barrett and T. Ikeda, *Angew. Chem., Int. Ed.*, 2008, **47**, 4986–4988; (*b*) T. Ikeda, J. I. Mamiya and Y. Yu, *Angew. Chem., Int. Ed.*, 2007, **46**, 506–528.
10 M. Poprawa-Smoluch, J. Baggerman, H. Z. Huub, P. A. Maas, L. De Cola and A. M. Brouwer, *J. Phys. Chem. A*, 2006, **110**, 11926–11937.
11 S. Sando, H. Abe and E. T. Kool, *J. Am. Chem. Soc.*, 2004, **126**, 1081–1087.
12 J. Yoshino, N. Kano and T. Kawashima, *Chem. Commun.*, 2007, 559–561.
13 M. Han and M. Hara, *J. Am. Chem. Soc.*, 2006, **128**, 10951–10955.
14 L.-H. Liu, K. Nakatani, R. Pansu, J.-J. Vachon, P. Tauc and E. Ishow, *Adv. Mater.*, 2007, **19**, 433–436.
15 S. Sreejith, P. Carol, P. Chithra and A. Ajayaghosh, *J. Mater. Chem.*, 2007, **18**, 264–274.
16 K. Liang, M. S. Farahat, J. Pelstein, K.-Y. Law and D. G. Whitten, *J. Am. Chem. Soc.*, 1997, **119**, 830–831.
17 K. Liang, K.-Y. Law and D. G. Whitten, *J. Phys. Chem. B*, 1997, **101**, 540–546.
18 D. M. Junge and D. V. McGrath, *Chem. Commun.*, 1997, 857–858.
19 D. De Selms, C. J. Fox and R. C. Riordan, *Tetrahedron Lett.*, 1970, **10**, 781–783.
20 A. D. Becke, *J. Chem. Phys.*, 1993, **98**, 5648–5652.
21 C. Lee, W. Yang and R. G. Parr, *Phys. Rev. B*, 1988, **37**, 785–789.
22 M. J. Frisch, G. W. Trucks, H. B. Schlegel, G. E. Scuseria, M. A. Robb, J. R. Cheeseman, V. G. Zakrzewski, J. A. Montgomery, Jr., R. E. Stratmann, J. C. Burant, S. Dapprich, J. M. Millam, A. D. Daniels, K. N. Kudin, M. C. Strain, O. Farkas, J. Tomasi, V. Barone, M. Cossi, R. Cammi, B. Mennucci, C. Pomelli, C. Adamo, S. Clifford, J. Ochterski, G. A. Petersson, P. Y. Ayala, Q. Cui, K. Morokuma, D. K. Malick, A. D. Rabuck, K. Raghavachari, J. B. Foresman, J. Cioslowski, J. V. Ortiz, A. G. Baboul, B. B. Stefanov, G. Liu, A. Liashenko, P. Piskorz, I. Komaromi, R. Gomperts, R. L. Martin, D. J. Fox, T. Keith, M. A. Al-Laham,

C. Y. Peng, A. Nanayakkara, C. Gonzalez, M. Challacombe, P. M. W. Gill, B. G. Johnson, W. Chen, M. W. Wong, J. L. Andres, M. Head-Gordon, E. S. Replogle and J. A. Pople, *GAUSSIAN 98 (Revision A.9)*, Gaussian, Inc., Pittsburgh, PA, 1998.
23 (*a*) Y.-C. Lu, E. W.-G. Diau and H. Rau, *J. Phys. Chem. A*, 2005, **109**, 2090–2099; (*b*) C.-W. Chang, Y.-C. Lu, T.-T. Wang and E. W.-G. Diau, *J. Am. Chem. Soc*., 2004, **126**, 10109–10118.
24 M. Yang and Y. Jiang, *Phys. Chem. Chem. Phys*., 2001, **3**, 4213–4217.
25 K.-Y. Law, *J. Photochem. Photobiol., A*, 1994, **84**, 123–132.
26 D. Suresh, T. T. Lekshmana, K. G. Thomas, P. V. Kamat and M. V. George, *J. Phys. Chem*., 1993, **97**, 13260–13264.
27 H. Rau, in *Photochromism, Molecules and Systems*, ed. H. Dürr and H. Bouas-Laurent, Elsevier, Amsterdam, 2nd edn, 2003, ch. 4.
28 (*a*) E. J. Habron, D. A. Vicente and M. T. Hoyt, *J. Phys. Chem. B*, 2004, **108**, 18789–18792; (*b*) E. J. Habron, D. A. Vicente, D. H. Hadley and M. R. Imm, *J. Phys. Chem. A*, 2005, **109**, 10846–10853.

